Polariton effects in reflectance and emission spectra of homoepitaxial GaN

R. Stępniewski, K. P. Korona, A. Wysmołek, J. M. Baranowski, and K. Pakuła
Institute of Experimental Physics, Warsaw University, Hoża 69, PL-00-681 Warszawa, Poland

M. Potemski and G. Martinez
Grenoble High Magnetic Field Laboratory, MPI/FKF-CNRS, Boîte Postale 166X, F-38042 Grenoble Cedex 9, France

I. Grzegory and S. Porowski
High Pressure Research Center, Polish Academy of Sciences, Sokołowska 29/37, PL-01-142 Warszawa, Poland
(Received 10 April 1997; revised manuscript received 10 July 1997)

Reflectance and photoluminescence spectra of exciton polaritons in GaN homoepitaxial layers, grown by metalorganic chemical-vapor deposition on GaN single crystals, are reported. Polariton modes involving excitons A, B, and C, which correspond to split valence bands of Γ_9, Γ_7, and Γ_7 symmetries, are resolved. Energies of the transverse excitons are found to be, respectively: $E_{TA}=3.4767$ eV, $E_{TB}=3.4815$ eV and $E_{TC}=3.4986$ eV, at the temperature $T=1.8$ K. The shape of the measured emission spectra depends upon donor concentration. This is explained in terms of interbranch polariton scattering. [S0163-1829(97)04448-2]

I. INTRODUCTION

In direct-gap semiconductors, there exists a strong coupling of free excitons with photons of similar energy. This phenomenon is essential for understanding the near-band-edge optical response, and has been studied in different materials such as, for example, GaAs (Refs. 1 and 2) or CdS.[3,4] Recently obtained high-quality homoepitaxial, i.e., unstrained, layers of gallium nitride[5] enable us to measure well-resolved reflectance spectra in the free-exciton energy region and, consequently, to study the polariton structure of GaN. Optical properties of this material are of a great interest due to the possible applications of GaN structures to short-wavelength optoelectronic devices. The paper is organized as follows: Section II is devoted to theoretical calculations of the polariton structure for hexagonal GaN. Both the polariton spatial dispersion and exciton excited states are included in a calculations within the dynamic dielectric function approximation. In Sec. III reflectance results are discussed. Kramers-Kronig analysis is applied to determine the near-band-edge absorption of the investigated GaN structures. Reflectance spectra observed in the experiment are compared with those resulting from calculations. The applied theoretical description, which includes the complete structure of the excited exciton states, allows us to reproduce the reflectance spectrum in the whole measured range. From the fitting procedure the band-structure parameters of GaN are derived. In Sec. IV, some detailed features observed in the luminescence spectra are discussed on the basis of the obtained polariton structure.

II. DISPERSION RELATIONS OF EXCITON POLARITONS IN GaN

Gallium nitride is a direct-band-gap semiconductor that crystallizes in the wurtzite structure. It is generally accepted that the top of the valence band is of Γ_9 symmetry, as in CdS.[6] Three excitons A, B, and C, which correspond to the split valence bands of Γ_9, Γ_7, and Γ_7 symmetries, respectively, can be observed in reflectance.[7–12] In GaN the crystal field and spin-orbit splitting parameters are significantly smaller[12] as compared to those of CdS.[6] In order to properly describe the optical constants that determine the measured spectrum, the different excitons cannot be treated separately, as in CdS,[13] but the simultaneous coupling of an electromagnetic wave with the A, B, and C excitons has to be taken into account. In the case of exciton-photon interaction, the dielectric function can be calculated by solving the coupled equations:[14]

$$\omega_X=\omega_{TX}+\frac{\hbar k^2}{2M}, \tag{1}$$

$$\frac{\partial^2 P}{\partial t^2}+\omega_X^2 P=\omega_X^2\alpha_X E-\gamma_X\frac{\partial P}{\partial t}, \tag{2}$$

$$\varepsilon^*\frac{\partial^2 E}{\partial t^2}-c^2\Delta E=-4\pi\frac{\partial^2 P}{\partial t^2}, \tag{3}$$

where E is the photon electric field and P is the polarization contribution due to the exciton. Equation (1) describes the center-of-mass motion of the free exciton with the wave vector k and the mass $M=m_e+m_h$. Equation (2) represents the excitonic oscillator coupled with a photon electric field through polarizability α_X. The frequency of the oscillator is ω_X and the damping constant is γ_X. Equation (3) describes the electromagnetic wave in a material for which the residual dielectric function is $\varepsilon^*(\omega)$.

Equations (1) and (2) take into account only the ground state of an exciton. On the other hand, the Kramers-Kronig analysis of the reflectivity data (see Sec. III) shows that for GaN an additional broadband absorption, arising from one-particle band-to-band transitions, occurs. The influence of the exciton excited states and transitions to the continuum can be included in the residual dielectric function $\varepsilon^*(\omega)$ in Eq. (3). Thus, it was assumed that

 © 1997 The American Physical Society

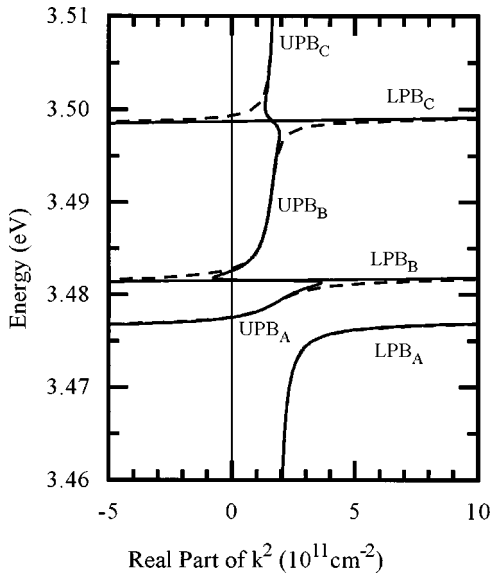

FIG. 1. Solid line: the calculated polariton dispersion curves of GaN. Four branches arising from photon coupling with A, B, and C excitons are labeled: LPB_X for the lower polariton branch of exciton X, and UPB_X for the upper polariton branch of exciton X. Three excitons lines originate from the crystal-field and spin-orbit splitting of the valence band. For comparison, curves calculated for $\gamma_X=0$ are plotted with a dashed line.

$$\varepsilon^*(\omega)=\varepsilon_0^*+\sum_{n=2}^{\infty} f_n \frac{\omega_n^2}{\omega_n^2-\omega^2-i\delta\omega} + \int_{E_{\mathrm{gap}}}^{E_{\max}} f_s \frac{\omega_s^2 ds}{\omega_s^2-\omega^2-i\delta\omega}. \tag{4}$$

For the excited states the energies are: $\hbar\omega_n=E_{\mathrm{gap}}-G/n^2$, where G is the exciton binding energy. The amplitudes f_n and f_s are calculated according to Elliott's formulas [Eq. (3.8) from Ref. 15 for excited states and Eq. (3.11) for continuum states].

Since free excitons in GaN involve valence-band holes that originate from the crystal-field and spin-orbit split valence band, we expect the existence of three exciton branches A, B, and C. It means that instead of the Eq. (1) we have to consider three equations for each exciton A, B, and C with corresponding frequencies ω_A, ω_B, and ω_C. Similarly, Eq. (2) is replaced by a set of three equations where we introduce three damping constants γ_A, γ_B, and γ_C and three different polarizabilities α_A, α_B, and α_C. Equation (3) is also modified. The polarization P is replaced by the sum of polarization contributions P_A, P_B, and P_C related to excitons A, B, and C, respectively. In the residual dielectric function $\varepsilon^*(\omega)$ the contributions from all excitons were included.

The calculated polariton dispersion curves of GaN obtained from the above-introduced polariton model are presented in Fig. 1. Dispersion curves are shown in energy versus k^2 coordinates. Four branches arising from photons coupled to A, B, and C excitons are labeled LPB_X (lower polariton branch of exciton X) and UPB_X (upper polariton branch of exciton X). The calculated dispersion relations presented in Fig. 1 have been obtained assuming parameters that result from the fit to the measured reflectance spectra (see Sec. III). It is worth noticing that values of damping constants γ_X are rather high and, therefore, a significant change in the shape of the dispersion curves is observed as compared to the $\gamma_X=0$ limit (shown with broken lines in Fig. 1). This is particularly visible for the C exciton for which damping is so strong that the exciton-photon coupling is hardly resolved.

In the case of a single exciton resonance, the reflectivity is easily defined assuming Fresnel boundary conditions, but when more than one polariton branch exists, the incident electromagnetic wave will excite more than one polariton wave with different wave vectors. In order to relate the phases and amplitudes of these polariton waves, additional boundary conditions are required. Here, we apply the approach first proposed by Pekar,[16] i.e., we assume that for each exciton X, its polarization contribution vanishes at the surface: $P_X=0$. In the following the effective index of refraction n_{eff} is introduced:[4]

$$n_{\mathrm{eff}}(\omega)=\sum_j n_j(\omega)E_j(\omega) \Big/ \sum_j E_j(\omega), \tag{5}$$

where the complex refractive index $n_j(\omega)$ and the electric-field amplitude $E_j(\omega)$ describe the propagation of the polariton j. According to the imposed boundary conditions, the excitons are excluded from a surface layer of thickness d (the so called dead layer). As a consequence, the reflectivity is a function of two interfering waves with the phase difference $\Theta=2kn_0d$ and is given by

$$R(\omega)=\left|\frac{n_s(\omega)-1}{n_s(\omega)+1}\right|^2, \tag{6}$$

calculated with the complex refractive index n_s defined as[3]

$$n_s=n_0\frac{(n_{\mathrm{eff}}+n_0)+(n_{\mathrm{eff}}-n_0)\exp(i\Theta)}{(n_{\mathrm{eff}}+n_0)-(n_{\mathrm{eff}}-n_0)\exp(i\Theta)}, \tag{7}$$

where $n_0=\sqrt{\varepsilon_0^*}$ is the residual (i.e., when neglecting excitonic resonances) refractive index.

III. REFLECTANCE DATA AND KRAMERS-KRONIG ANALYSIS

For our experiments, homoepitaxial GaN layers were used. The GaN crystals, used as substrates, were grown by the high-pressure method.[17] These crystals have the form of platelets with the hexagonal **c** axis perpendicular to the surface. Our substrate material is characterized by an electron concentration of about 10^{19} cm^{-3}. Platelets with fairly flat surfaces (of about 10 mm^2) were chosen for the metal-organic chemical-vapor depostion (MOCVD) growth. The GaN substrates, before the epitaxial process, were etched in the boiling *aqua regia* and rinsed in deionized water. The layers were grown in a horizontal atmospheric pressure system adapted for the growth of nitrides. The trimethylgallium and NH_3 were used as sources of Ga and N, respectively, in addition to hydrogen as a carrier gas. GaN layers were grown

at a temperature close to 1000 °C, directly on single crystals substrates without deposition of a nucleation layer at low growth temperature. The layer thickness was about 1 μm. Due to the high substrate conductivity the layers could not be characterized by the electrical transport measurements. Detailed properties of our GaN homoepitaxial layers are reviewed in Refs. 18 and 19. For optical measurements, the sample was immersed in a bath of liquid helium. For the reflectance measurements we chose the epitaxial layer with the best surface quality (i.e., the sample with the largest smooth area). Experiments were performed at 1.8 K using optical fibers with ends mounted in front of the sample. The angle of incidence was set to 30 °. In the case of the semiconductors with the wurtzite structure the uniaxial symmetry can strongly affect the selection rules of the optical transitions. Since the optical transition between the valence band of the Γ_9 symmetry and the conduction band (Γ_7 symmetry) is allowed for the polarization $\vec{E}\perp\vec{c}$, this effect is particularly important in the case of samples with the hexagonal axis parallel to the sample surface. For this particular configuration, typical for the CdS crystals, the reflectance spectrum is influenced by the incident light direction and polarization.[3,13] In the case of homoepitaxial GaN layers the hexagonal axis is perpendicular to the sample surface and these effects are not so important. Therefore, for simplicity, the off normal direction of the incident light, present in our experiment, will be neglected henceforth.

The spectral resolution of the monochromator was 0.2 meV. Reflectance spectra were scaled with respect to the reflectivity of aluminum and derived from the ratio of the reflection signals measured from the sample and from the aluminum mirror. The reference reflection spectrum was measured at room temperature but with the same experimental setup in which only the sample was replaced by a small aluminum mirror. The reflectivity of aluminum was assumed to be 0.92 in the spectral range considered.[20]

The low-temperature near-band-edge reflectance spectrum of GaN is shown in Fig. 2(a). This spectrum allows us to clearly distinguish three dispersion lines. Such characteristic spectra have been reported previously[7–12] and are assigned to the excitonic resonances. They directly reflect a typical wurtzite-type valence-band structure of GaN, which consists of three valence bands of the Γ_9, Γ_7, and Γ_7 symmetry, respectively. According to the polariton model described in Sec. II we have calculated the corresponding reflectance spectrum and fit it to the experimental data [see Fig. 2(a)].

Up to now, the fine structure of the excited states for the free excitons A, B, and C in GaN is not known in detail. On the other hand, the calculated reflectance spectrum is sensitive to the value of the binding energy of the A exciton only. Therefore, the exciton binding energies for excitons A, B, and C were assumed to be the same ($G_A=G_B=G_C=G$). Similarly, the exciton masses have been set to be[10] $M=m_0$ (m_0 is the bare electron mass). The exciton energies E_{TX}, the linewidths γ_X, polarizabilities $4\pi\alpha_X$, as well as the dead layer thickness d, the exciton binding energy G, and the broadening parameter δ have been used as fitting parameters. The best fit values of E_{TX}, γ_X, and α_X are given in Table I.

The exciton-photon coupling is sometimes described by the longitudinal-transverse splitting:[14]

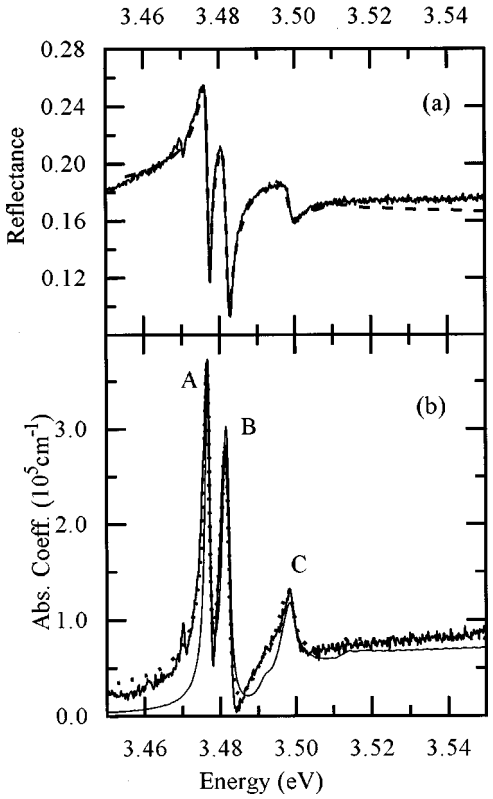

FIG. 2. (a) The experimental reflectance spectrum of a GaN layer at $T=1.8$ K, solid line, and the fitted theoretical curve, dashed line; (b) the absorption coefficient derived by the Kramers-Kronig analysis, solid line; obtained from the exciton-polariton model fitted to the reflectance data [Eq. (6)], dotted line, and expected ''bulk'' absorption, solid thin line.

$$\Delta_{LTX}=E_{TX}\left(\sqrt{1+\frac{4\pi\alpha_X}{\varepsilon^*}}-1\right)\approx E_{TX}{*}4\pi\alpha_X/(2\varepsilon^*), \tag{8}$$

The calculated values of Δ_{LTX} corresponding to the free excitons A, B, and C are also presented in Table I.

For the other parameters we have obtained $E_{\mathrm{gap}}=E_A+G=3.497$ eV, $\varepsilon_0^*=5.2$, $\delta=5$ meV, and $d=4.1$ nm, which is close to the expected exciton diameter. As shown in Fig. 2, the measured reflectance is well reproduced by calculations. A small discrepancy between the calculated curve and experimental data exists in the energy range from 3.455 eV to 3.475 eV (the region of bound excitons), and above the excitonic structures. This can be related to the additional dispersion of the real part of the dielectric function, induced by a strong absorption (for $\hbar\omega>5$ eV) present in GaN,[21] but not included in our calculations.

Our analysis is quite accurate, particularly when estimating the excitonic energies. It should be noted that in the case of homoepitaxial GaN layers the changes in the exciton energies from sample to sample (related to possible residual strain) are rather small (less than 2 meV).[22,9] Hence, our results, though obtained for a particular sample, give a fairly reliable estimation of exciton energies in hexagonal GaN. The obtained exciton energies can be used to estimate the

TABLE I. Parameters of exciton polaritons in hexagonal GaN obtained from the analysis of the near-band-edge reflectance spectrum.

Exciton: X	Energy $E_{TX}=\hbar\omega_X$ (meV)	Linewidth $\Gamma_X=\hbar\gamma_X$ (meV)	Polarizability $4\pi\alpha_X$	Longitudinal-transverse splitting (meV)
A	3476.7 ± 0.3	0.7 ± 0.2	$(2.7\pm0.3)\times10^{-3}$	0.90 ± 0.10
B	3481.5 ± 0.3	1.5 ± 0.2	$(3.1\pm0.3)\times10^{-3}$	1.04 ± 0.10
C	3498.6 ± 0.8	3.1 ± 0.8	$(1.1\pm0.3)\times10^{-3}$	0.37 ± 0.10

parameters that describe the valence-band splitting. Applying Hopfield's quasi cubic model[23] we obtained spin-orbit splitting, $\Delta_{so}=(17.9\pm1.2)$ meV and crystal-field splitting, $\Delta_{cr}=(8.8\pm0.8)$ meV. These values are compared in Table II to the previously estimated by different authors,[7–11] on the basis of the reflectivity measurements of the GaN layers grown on different lattice mismatched substrates such as sapphire. While in the case of the spin-orbit splitting one can notice similar results, the values obtained for the crystal-field splitting are quite different, since this parameter value is strongly affected by strain. The data obtained for GaN homoepitaxial layers and reported here might be used as a reference to determine the shift of excitonic resonances in heteroepitaxial layers.

The polarizabilities of excitons in GaN (see Table I) can be compared with the corresponding values ($4\pi\alpha_0$) reported for GaAs,[1] CdS,[2] or ZnO.[2] The exciton-photon coupling is stronger in GaN than in GaAs ($4\pi\alpha_0=0.0012$) but definitely weaker than in II-VI compounds ($4\pi\alpha_0=0.014$ for CdS and $4\pi\alpha_0=0.0077$ in the case of ZnO). This is what one could expect, since GaAs is a more covalent compound whereas II-VI materials show more ionic character than GaN.

The appropriate analysis of the reflectance spectrum allows us to reconstruct the corresponding absorption spectrum. We have derived the absorption spectrum applying two different methods. First, the measured reflectance spectrum has been transformed into the absorption one using the Kramers-Kronig relations.[24] Second, we have simply calculated the absorption spectrum from the already known parameters of the polariton structure deduced from the fit to the reflectance data. It is required for the Kramer-Kronig analysis that the transformed spectra be known over a wide frequency range. Our data cover a rather narrow spectral range (3.43 eV–3.55 eV). For energies above the measured range (up to 30 eV) the data available in the literature[21] have been used in order to reconstruct the corresponding spectrum. Additionally, we assumed that for the energy range of 0 eV–3.43 eV there is no absorption present in GaN (we neglect the absorption processes due to phonons that exist below 0.1 eV). Applying this assumption, the reflectance for energies below the measured range was extrapolated numerically.[25] The absorption coefficient derived from Kramer-Kronig analysis of the reflectance is shown in Fig. 2(b) with a solid line. The dotted curve presented in the same figure represent the ''surface'' absorption coefficient $\alpha_s=(2\omega/c)\cdot\mathrm{Im}(n_s)$, calculated directly from the polariton model, including the dead layer effect (Eq. 7), with parameters previously used to reproduce the reflectance spectra. As can be seen in Fig. 2(b), both methods give very similar results. They are slightly different than the expected ''bulk'' absorption coefficient $\alpha_{\mathrm{eff}}=(2\omega/c)\cdot\mathrm{Im}(n_{\mathrm{eff}})$ [Eq. (5)], which can be applied to reconstruct the fundamental absorption edge in the investigated sample [Fig. 2(b), solid thin line]. As shown in Fig. 2(b), the absorption spectrum of the investigated GaN layer displays three dominant structures A, B, and C, with peaks at energies that correspond to the exciton energies E_{TA}, E_{TB}, and E_{TC}, respectively. One can also distinguish the steplike absorption band that sets on around 3.49 eV and that is ascribed to an absorption continuum corresponding to the valence-band–conduction-band transitions. It is interesting to note that in addition to the strong lines due to the free excitons there is also a weak structure at 3.471 eV, attributed to a donor bound exciton (note the corresponding feature in the reflectance spectrum). This observation indicates a strong oscillator strength of the donor bound exciton in GaN. Transitions related to bound excitons are rarely observed in the reflectance spectra, though such an observation has been already reported for CdS.[26]

TABLE II. The crystal-field splitting, Δ_{cr}, and the spin-orbit splitting, Δ_{so}, parameters in the wurtzite GaN, within cubic approximation, obtained by different authors.

Δ_{cr} (meV)	Δ_{so} (meV)	
22	11	Dingle *et al.*[a]
72.9	15.6	Suzuki *et al.*[b]
10.0 ± 0.1	17.6 ± 0.3	Gil *et al.*[c]
35	18	Volm *et al.*[d]
11	17	Volm *et al.*[e]
22	15	Shikanai *et al.*[f]
8.8 ± 0.8	17.9 ± 1.2	This work

[a]Reference 7.
[b]Reference 8.
[c]Reference 9.
[d]Reference 10—''without strain.''
[e]Reference 10—''relaxed film.''
[f]Reference 11.

IV. FREE-EXCITON LUMINESCENCE

As free excitons are commonly investigated using emission spectroscopy it is interesting to confront the proposed exciton-polariton model deduced from the analysis of the reflectivity data with the corresponding luminescence spec-

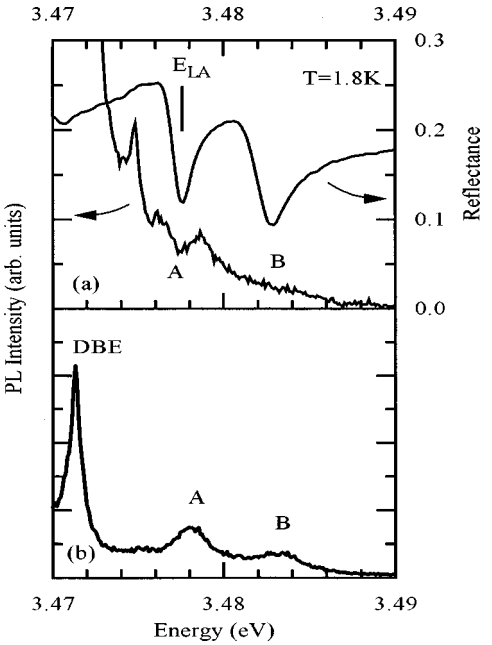

FIG. 3. Photoluminescence and reflectance spectra of homoepitaxial GaN. Photoluminescence spectra shown in (a) and (b) have been measured for samples with different donor concentrations.

tra. The comparison of the reflectivity and luminescence spectra measured on the same sample is shown in Fig. 3(a). The photoluminescence spectrum, observed for this sample, is rather typical for our homoepitaxial layers,[5,12] and have been discussed previously. Although the recombination related to the bound excitons[27] is very strong, clear emission traces are also observed in the range of the free-exciton emission. For further discussion, an important observation is a doublet emission structure clearly visible in the region of the exciton A. As shown in Fig. 3(a), the energy of the longitudinal exciton E_{LA} (Ref. 28) falls roughly in the middle between the two components of the exciton A emission doublet. On the other hand, the emission spectrum displayed in Fig. 3(b) shows one peak at an energy above the reflectivity minimum. As can be deduced from the relative intensities of the luminescence lines, these two homoepitaxial layers differ in the donor concentration. For the first sample the intensity of the emission related to the donor bound exciton (DBE) as compared to that of the free exciton is very high (a ratio of about 100), which indicates a relatively high concentration of donors in this unintentionally doped sample. For the second layer the ratio of the intensity of DBE to that of the free exciton is close to 4 and, therefore a smaller concentration of donors is expected.

The observed differences between emission spectra shown in Figs. 3(a) and 3(b) can be qualitatively understood. On the lower polariton branch (LPB) (see Fig. 1), at large wave vectors, the polaritons are predominantly excitonlike. On the upper polariton branch (UPB), above the resonance the polaritons are photonlike with increasing wave vector. The polariton dispersion has a profound effect on the luminescence mechanism due to the polariton scattering process. In the case of lightly doped samples, processes with phonon emission dominate but are not efficient for polaritons with small wave vectors (the bottleneck effect).[14] In addition, the interbranch scattering from the LPB_A to the UPB_A photonlike region of the dispersion curve may take place as well. The polariton luminescence results from those polaritons which, upon reaching the surface, are converted into photons leaving the crystal. The polaritons from the UPB_A have a more photonlike character and provide a path for polaritons to escape the crystal. Therefore the luminescence from the energy region above E_L is primarily from the UPB_A. In addition, in GaN, the polariton branch connected with exciton B (LPB_B) merges into the polariton branch UPB_A (see Fig. 1). This may create an effective path for polaritons to be scattered to UPB_A. As a consequence, there may be expected a single emission peak, at an energy above the reflectivity minimum, such as the one shown in Fig. 3(b).

However, a more common feature, not only in homoepitaxial GaN layers but also in other semiconductors, is a doublet structure such as shown in Fig. 3(a). As discussed in Ref. 1, the neutral donor elastic scattering for polaritons is essential for the observation of the emission contributions from both polariton branches. Therefore, a high concentration of donors may create a way for polaritons to be efficiently scattered to the LPB_A at the bottleneck energy, at which they finally reach the surface and convert themselves into photons. Such an effect was observed in GaAs where, depending on the neutral donor concentration, a single or a double peak was observed.[1]

V. CONCLUSIONS

The reflectivity and luminescence of high-quality homoepitaxial gallium nitride layers have been presented. We have shown that the reflectivity spectrum of GaN can be reproduced in detail taking into account exciton polaritons associated with the complex valence-band structure, as well as absorption processes related to the band-to-band continuum. The polariton model of emission qualitatively accounts for the changes in the shape of the free-exciton emission in samples with different donor concentrations. However, it should be pointed out that the polariton effects in the free-exciton emission are difficult to interpret quantitatively because they are connected with scattering of polaritons within the layer of the crystal excited by light. On the other hand, it is relatively easy to include polariton effects in the analysis of reflectivity data which are free from the relaxation problem.

ACKNOWLEDGMENTS

The authors would like to express their gratitude to the SEZAM program organized by the Foundation for Polish Science, thanks to whose help they could purchase the scrubbing system for the MOCVD reactor. This research was partially supported by State Committee for Scientific Research (Republic of Poland) Grant No. 7 T08A 06110 and French-Polish Scientific Cooperation Project No. 6447. The GHMPL is ''laboratoire associé avec l'INPG et l'UIF de Grenoble.''

[1] T. Steiner, M. L. W. Thewalt, E. S. Coteles, and J. P. Salerno, Phys. Rev. B **34**, 1006 (1986).
[2] D. Sell, S. E. Stokowski, R. Dingle, and J. V. DiLorenzo, Phys. Rev. B **7**, 4568 (1973).
[3] J. J. Hopfield and D. G. Thomas, Phys. Rev. **132**, 563 (1963).
[4] J. Lagois, Phys. Rev. B **16**, 1699 (1977).
[5] K. Pakuła, A. Wysmołek, K. P. Korona, J. M. Baranowski, R. Stępniewski, I. Grzegory, M. Boćkowski, J. Jun, S. Krukowski, M. Wróblewski, and S. Porowski, Solid State Commun. **97**, 919 (1996).
[6] D. G. Thomas and J. J. Hopfield, Phys. Rev. **116**, 573 (1959).
[7] R. Dingle, D. D. Sell, S. E. Stokowski, and M. Ilegems, Phys. Rev. B **4**, 1211 (1971).
[8] M. Suzuki, T. Uenoyama, and A. Yanase, Phys. Rev. B **52**, 8132 (1995).
[9] B. Gil, O. Briot, and R. L. Aulombard, Phys. Rev. B **52**, R17 028 (1995).
[10] D. Volm, K. Oettinger, T. Streibl, D. Kovalev, M. Ben-Chorin, J. Diener, B. K. Meyer, J. Majewski, L. Eckey, A. Hoffman, H. Amano, and I. Akasaki, Phys. Rev. B **53**, 16 543 (1996).
[11] A. Shikanai, T. Azuhata, T. Sota, S. Chichibu, K. Horino, and S. Nakamura, J. Appl. Phys. **81**, 417 (1997).
[12] K. P. Korona, A. Wysmołek, K. Pakuła, R. Stępniewski, J. M. Baranowski, I. Grzegory, B. Łucznik, M. Wróblewski, and S. Porowski, Appl. Phys. Lett. **69**, 788 (1996).
[13] I. Broser, M. Rosenzweig, R. Broser, M. Richard, and E. Birkicht, Phys. Status Solidi B **90**, 77 (1978); M. Rosenzweig, *ibid.* **129**, 187 (1985).
[14] S. Nakajima, Y. Toyozawa, and R. Abe, *The Physics of Elementary Excitations* (Springer-Verlag, Berlin, 1980).
[15] R. J. Elliott, Phys. Rev. **108**, 1384 (1957).
[16] S. I. Pekar, J. Phys. Chem. Solids **5**, 11 (1958).
[17] S. Porowski, J. Jun, M. Boćkowski, M. Leszczyński, S. Krukowski, M. Wróblewski, B. Łucznik, I. Grzegory, in *Proceedings of the 8th Conference on Semi-Insulating III-V Materials, Warsaw 1994*, edited by M. Godlewski (Word Scientific, Singapore, 1994), p. 61.
[18] J. M. Baranowski and S. Porowski, in *Proceedings of the 23rd International Conference on the Physics of Semiconductors, Berlin 1996*, edited by M. Sheffler and R. Zimmermann (World Scientific, Singapore, 1996), p. 497.
[19] R. Stępniewski and A. Wysmołek, Acta Phys. Pol. **90**, 681 (1996).
[20] C. J. Powell, in *Numerical Data and Functional Relationships in Science and Technology*, edited by K. -H. Hellwege and J. L. Olsen, Landolt-Börnstein, New Series, Group III, Vol. 15, Pt. b, (Springer-Verlag, Berlin, 1985), p. 228.
[21] S. Logethetidis, J. Petlas, M. Cardona, and T. D. Moustakas, Phys. Rev. B **50**, 18 017 (1994).
[22] M. Leszczyński, H. Teisseyre, T. Suski, I. Grzegory, M. Boćkowski, J. Jun, S. Porowski, K. Pakuła, J. M. Baranowski, C. T. Foxon, and T. S. Cheng, Appl. Phys. Lett. **69**, 73 (1996).
[23] J. J. Hopfield, J. Phys. Chem. Solids **15**, 97 (1960).
[24] F. Stern, in *Solid State Physics*, edited by F. Seitz and D. Turnbull (Academic, New York, 1963), Vol. 15, p. 341.
[25] K. Jezierski, J. Phys. C **17**, 475 (1984).
[26] K. Bohnert, G. Schmieder, S. El-Dessouki, and C. Klingshirn, Solid State Commun. **27**, 295 (1978).
[27] Dominated luminescence lines (not shown in Fig. 3) are the excitons bound to the neutral acceptor and neutral donor (discussed in Ref. 5), observed for this sample at $E_{XA}=3.4568$ eV, $E_{XD}=3.4713$ eV, respectively. The origin of the weaker line, also related to the donor bound exciton, visible in Fig. 3. at $E_a=3.4748$ eV, is discussed in Refs. 5 and 10.
[28] The energy positions of the longitudinal excitons $E_{LX}\approx E_{TX}[1+4\pi\alpha_X/(2\varepsilon^*)]$ correspond to the minima in the reflectivity and these energies can be relatively well determined even from the raw spectra.